Received: November 25, 2021. Revised: January 19, 2022. 36

International Journal of
Intelligent Engineering & Systems

http://www.inass.org/

Optimal Fractional Order PID Controller Design of Bidirectional DC-DC Converter Using Falcon Optimization Algorithm

Umasankar Loganathan[1]* Charles Rajeswaran[1]
Harindrakumar Jayaraj[1] Manoj Magesh[1]

[1]*Department of Electrical and Electronics Engineering, RMK College of Engineering and Technology, Puduvoyal, Chennai, India*
* Corresponding author's Email: haripriyathirumarai@gmail.com

Abstract: In the present scenario, the DC-DC converter becomes the most significant device and it is used in various applications such as Electric vehicles, fuel cells, sustainable systems, etc. A bidirectional converter used in the above-mentioned applications should be lesser in magnitude and lighter in weight. In case, if the magnitude of the traditional bidirectional DC-DC converter is more, the substituting consistency has been amplified that results in more switching losses. Because of this switching loss, the magnitude of the structure is minimized. To overcome the losses during the process, a novel topology of dc-dc converters is designed with Falcon Optimization Algorithm (FOA) to increase the efficiency of converters. This research proposes the design of Bidirectional DC-DC converter (BDDCDC) for C and π Filter through Fractional Order Proportional Integral Derivative (FOPID) which is tuned by FOA. This proposed controller synthesis considers both robustness and closed-loop performance to ensure a fast and stable regulation characteristic. A simple tuning method provides the appropriate gains to meet design requirements. The outcomes of proposed FOA-FOPID is simulated in MATLAB Simulink which represent the transient performances such as steady state error (1.1 V), rise time (0.21 sec), settling time (0.33 sec) and peak time (0.24 sec) is much better than existing PID and Adaptive Neuro Fuzzy Inference System (ANFIS) control.

Keywords: Bi-directional converter, C and π filter fractional order proportional integral derivative, Proportional integral, Voltage ripple.

1. Introduction

Currently, Bi-Directional DC-DC regulators are commonly used to transform the power from the dual DC sources, which operate with steadied output voltage [1-3]. Conventionally, Proportional Integral (PI) and PI Derivative (PID) controllers proceed towards the supreme regulators [4] along with an enormous quantity of electrical components. The capability of the converter in the buck/boost mode has been analysed through various topology and circuit organizations [5, 6]. Specifically, during the entire reestablishment diode phase, diodes could be activated by electromagnetic disruption difficulties on account of unnecessary current flows [7]. Previously developed controllers like PI, PID and fuzzy are exploited for the speed and torque ripple reduction in the load side. [8].

In view of the constant expansion and development of the social order, the day-to-day manufacture and lifespan requirement for bidirectional converters is progressively growing [9]. The DC-DC converter is extensively exploited for the reason that it can comprehend the bidirectional movement of power and collects information about unidirectional converters [10, 11]. Moreover, the converter accomplishes more rapid and active performance over double unidirectional DC-DC converters [12]. At the moment, bidirectional DC-DC is being extensively utilized in energy systems and microelectronic eliminations [13]. This controller technique frequently leads to fragile controller strength, and there is inconsistency present in the

overshoot & regulation time of the configuration [14]. The main advantage of proposed FOA-FOPID controller is that it provides more adjustable time and frequency responses of the control system allowing fulfilment of better as well as robust performance. Furthermore, this proposed method is easy to implement, deliberating the quality parameters and compatible with nearby modules. The main contributions of the work are mentioned as follows,

- Design and analysis of Bidirectional DC-DC converter (BDDCDC)
- After designing the DC-DC converter, the process is validated with various controllers.
- Finally, the converter is designed with FOA-FOPID controller which produces better results when compared with other PID controllers.

The research paper is organized in the following manner: The literature review of this work is described in Section 2. Section 3 describes the workflow of the proposed method and its converter operation. Section 4 provides the results and discussions of the proposed FOA-FOPID controller. Finally, the conclusion is made in Section 5.

2. Literature review

Brajesh Kumar [15] has demonstrated a closed loop control of PID controller to DC-DC converter in the existence of load variations and noises. The novelty of this paper lies in the design of modified PID controller to track the reference trajectory with and without load in addition to minimizing the initial overshoot. Although, this proposed method cannot accomplish adequate determination to overcome this dissimilarity in extended intervals.

Subramanian [16] has proposed a reduction of quantum vibration and maintain the drives by using DPCT control. The inverter is utilized here to run the motor in a steady speed process. This DPCT is substituting to traditional cascaded technique in current and speed regulation of motor drives. The input current of inverter is openly regulating by means of DPCT method. While, the reference design precision was not assured to the variation of BLDC constraints.

Suryoatmojo Heri [17] demonstrated the transient control of drives via Adaptive Neuro Fuzzy Inference System (ANFIS). Also, this proposed method proceeds with less interval to accomplish steady state error. With the help of proposed ANFIS, rise time gets reduced and create the model as quicker. The proposed ANFIS method has a superior preliminary torque and current when associated with existing methods. But, considering control rule cases, contrasting controller behaviour produces inferior outcome sooner.

Vanchinathan [18] demonstrated a model to proceed a simulation for motor speed regulation through Modified Genetic Algorithm based Fractional Order PID (MGA-FOPID) controller. The proposed MGA-FOPID is verified under various load and speed conditions to validate the results. Then this proposed algorithm is beneficial for reducing the performance indexes. However, the exploiters torque has a substantial overshoot and extensive error rate when compared with other algorithms.

AL-Mawlawe [19] has developed a fuzzy rule dependent technique for controlling the buck-boost converter. The major aim of this method is to model and validate a fuzzy method which regulates the duty cycle of the converter operating in uninterrupted manner. The assessment of the voltage is associated to improve the presentation of the system which confirms an energetic reaction and delivers steady voltage. However, the issue of recognizing the proper membership functions for fuzzy structures are still presented over there.

Aguila-Leon [20] has demonstrated the Grey Wolf Optimization for the control of transient performance in DC-DC boost converter. The proposed GWO algorithm is a feasible solution for the PID controller tuning problem for power converters since its overall performance is better than the results obtained by the PSO and GA. However, the PID tuned through the GWO was a little slower to reach the reference voltage than the other algorithms.

2.1 Solution:

It is difficult to tune the parameters and get satisfied control characteristics by using normal conventional PID controller. Here, FOA-FOPID controller with novel dc-dc topology is proposed with adaptation special quality and soft control performance outside than traditional controller. As it has the ability to satisfied control characteristics and easy for computing.

3. Proposed method

Initially, the power is extracted from the DC source which acts as a primary source supply. Through the supply, DC-DC converter is connected which is exploited to convert the voltage from variable dc into fixed dc. In that converters, switches are presented that switch is triggered by the Pulse Width Modulation (PWM) pulses. Then a high-frequency transformer is integrated into between the

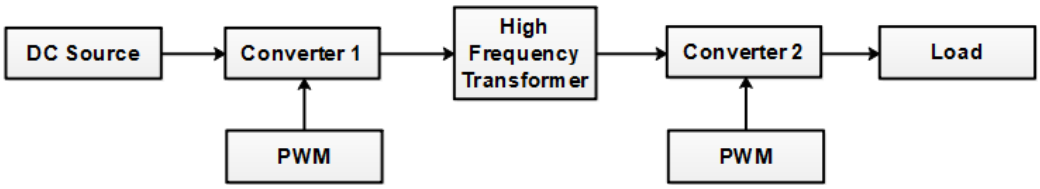

Figure. 1 Overview of proposed model

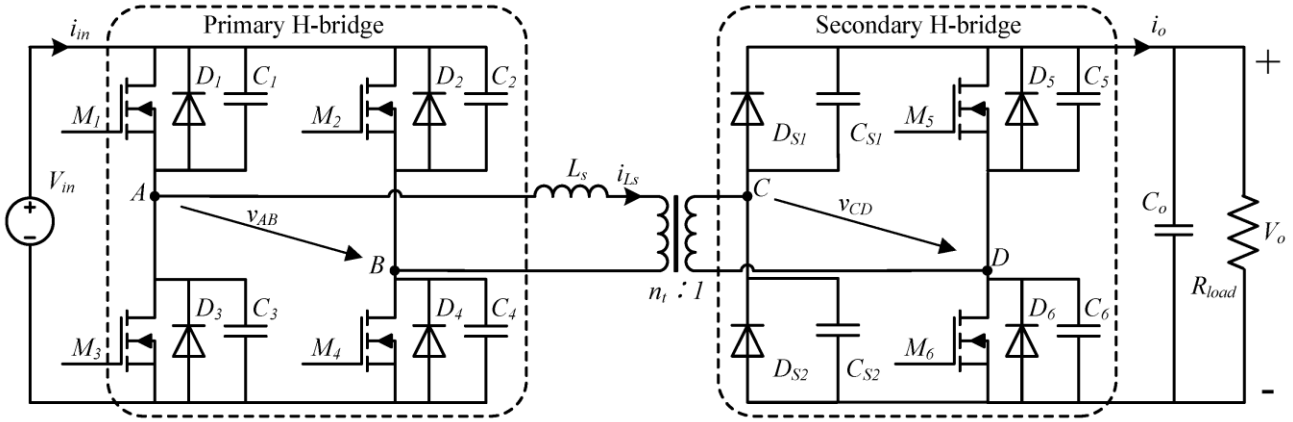

Figure. 2 Design circuit of proposed converter

two bidirectional DC-DC converters. The bidirectional DC/DC converter comes from the common unidirectional DC/DC converter and can achieve energy flow in two directions. Electronic equipment in markets cannot work without a stable power supply system. With the development of technology, the number of types of electronic products is steadily increasing. The stability of the power supply system is key to guaranteeing good working conditions in electronic production. Moreover, the performance of the power supply directly influences the safety and stability of electronic equipment. This study achieves bidirectional transmission of energy by rational hardware design of a bidirectional DC/DC converter and improves the reliability of the system. The proposed method provides a good prospect of a control scheme for the bidirectional DC/DC converter to optimize practical engineering design.

A typical application for this converter is battery charging for electrical vehicles, telecommunication and speed control of dc-motor. The advantages of the circuit with c filter are reduced ripple content present in the voltage/current waveforms, soft switching, low cost and high efficiency. The results of the bidirectional DC-DC converters are compared with C and π filter design. The filter decreases the swells existent in the converter output. The usage of fractional order with designed DC-DC converter increase and simplify well-established controller approaches and strategies. FOA-FOPID has also been established to be proficient of overpowering disordered behaviours in measured simulations. The

Table 1. Ratings of proposed converter

Components	Ratings
Switching frequency	100 kHz
Transformer turns ratio	1:4
Capacitance C1, C2	220mF
Magnetizing inductance L1	21.22mF
Magnetizing inductance L2	331.18mF
Leakage inductance primary side	0.606 mF
Leakage inductance secondary side	15.059mF

major advancement of this proposed topology is mentioned as follows; This proposed converter topology does not require linearization because which depends on principal behaviour, that makes it insensitive to parameter variations. The switching (ON/OFF) decisions are based on current system state, so, mode transitions are possible in this proposed topology. Henceforth, to preserve the constant output voltage and current, FOA-FOPID controllers are executed in this research. Fig. 1 displays the block diagram of the proposed system and Fig. 2 displays the circuit diagram of the bidirectional DC-DC converter. Table 1 tabulates the specifications for the bidirectional DC-DC converter.

3.1 Falcon optimization algorithm

The proposed control system handles quadrant transitions well, as seen in the results section. The provided code can handle current control and voltage control. The device topology is fully bidirectional, and there were no problems changing direction of the power. The key motivation for the proposed procedure and specifics about its execution are

offered in this segment. The motivation of this calculation was the chase conduct of falcons when they are seeking after a prey in flight.

Stage 1: Initialize the enhancement issue, choice factors and limitations. Then, the adjustable parameters of FOA such as quantity of falcons (NP), maximum allowed speed (v_{max}), values of cognitive (C_c), social (S_c), following (S_c) constants and awareness and dive probabilities (AP, DP) are provided.

Stage 2: Initialize position and speed of the falcons. Then the birds are haphazardly situated in a D-dimensional space regarding the limit conditions, creating the lattice:

$$x = \begin{bmatrix} x_{1,1} \dots \dots x_{1,D} \\ . \\ . \\ . \\ x_{NP,1} \dots \dots x_{NP,D} \end{bmatrix} \quad (2)$$

where *x* is the falcon position, respecting the quantity of NP candidates in all its D dimensions. The velocities are randomly generated between v_{max} and v_{min} restrictions, where both are determinate respecting:

$$v_{max} = 0.1ub \quad (3)$$

$$v_{min} = -v_{max} \quad (4)$$

where v_{max} and v_{min} are the most extreme and least speeds permitted, individually, and ub is the upper bound breaking point scope of the issue for each measurement.

Stage 3: Evaluate wellness and discover worldwide and individual best situations for each falcon the fitness value for the issue is gotten, creating the vector:

$$OF = \begin{bmatrix} of_1 \\ . \\ . \\ . \\ of_2 \end{bmatrix} \quad (5)$$

Where, OF represents the objective fitness. Then, the best individual is set to be the g_{best} position and for each falcon its best individual position is set as x_{best}.

Stage 4: Generate new positions and update the falcon positions right away, two arbitrary numbers (P_{AP}, P_{DP}) are created, where in case P_{AP} is lower than the falcon plays out a development of looking for preys as per the its experience and the other falcon encounters:

$$x_{iter} = x_{iter-1} + v_{iter-1} + C_c r\left(x_{best,iter-1} - x_{iter-1}\right) + S_c r\left(g_{best,iter-1} - x_{iter-1}\right) \quad (6)$$

where x_{iter-1} and v_{iter-1} are the current position and speed of the falcon, separately. $C_c r$ is stated as cognitive rate; $S_c r$ is represented as social. Assuming P_{AP} is higher than AP (Adaptive Probability), the jump likelihood is contrasted and P_{DP}. Assuming P_{DP} is higher than DP (Dive Probability), the falcon targets one picked prey (x_{chosen}) and plays out its underlying development for hunting, the logarithmic twisting given by:

$$x_{iter} = x_{iter-1} \left|x_{chosen} x_{iter-1}\right| \exp(bt) \cos(2\pi t) \quad (7)$$

Where x_{iter} is the newly obtained position; b is a consistent characterizing the state of the logarithmic twisting, equivalents to 1, and t is an irregular number in the reach [−1, 1] that characterizes how much the following situation of the falcon would be near its genuine objective. Assuming P_{AP} is lower than P_{DP}, the wellness of the picked prey is contrasted with the wellness of the falcon where if the prey is fittest it will be trailed by the bird of prey, like a jump development:

$$x_{iter} = x_{iter-1} + v_{iter-1} + f_c r(x_{chosen} - x_{iter-1}) \quad (8)$$

Where, $f_c r$ is stated as following constant; If not, the falcon performs a movement according to its own individual best position,

$$x_{iter} = x_{iter-1} + v_{iter-1} + C_c r(x_{best,iter-1} - x_{iter-1}) \quad (9)$$

After, its new fitness values are registered and the new updates of g_{best} and x_{best} are gotten. Essential to see that in all method descripted in Step 4.

Stage 5: Finally, after every one of the assessments the cycle is proceeded until the most extreme number of ($iter_{max}$) in this manner rehashing the Step 4.

3.2 FOPID controller

Generally, PID controllers are calculated for bidirectional DC-DC converter which has more or less restrictions. To improve the DC-DC converters' transient response, in this research, a Fractional Order PID controller (FOPID) with novel dc-dc topology is

executed. The main advantage of Fractional-order controller is that it delivers supplementary adaptable time and frequency responses of the proposed system permitting accomplishment of improved as well as modest performance. The proportional, integral and derivative (PID) term is specified by the following Eq. (10) to (13),

$$P = K_p.e(t) \tag{10}$$

$$I = K_i \int_0^t e(\tau) d\,\tau \tag{11}$$

$$D = K_d \frac{de(t)}{dt} \tag{12}$$

$$PID = K_p.e(t) + K_i \int_0^t e(\tau) d\,\tau + K_d \frac{de(t)}{dt} \tag{13}$$

Tuning PID controller parameters (K_p, K_i, K_d) Where proportional controller gain is stated as (K_p), integral control gain is represented as (K_i), K_d characterizes the differential control gain, $e(t)$ signifies the new error signal, rate of change of error is stated as $\frac{de(t)}{dt}$, a changeable coefficient is described as τ.

The complete control operation is explained by the following Eq. (14),

$$m(t) = K_p e(t) + K_i \int e(t) dt \tag{14}$$

$m(t)$ represents the control signal, while in the s-domain, it is stated as Eq. (15),

$$M(s) = \left[K_p \frac{K_i}{S}\right] E(s) \tag{15}$$

The fractional orders are represented by λ and μ, where $E(s)$ signifies the error signal.

when K_p is at maximum, steady-state error gets decremented and speed of the system gets increased, but there is no elimination present in the system. There is an increment in the damping factor, and decrement in the overshoot when K_d is maximum. The error at the steady-state reaches nil and the structure leans in the direction of uncertainty when K_i is maximum; it shows that $PI^{\lambda}D^{\mu}$ control possibly will increase the performance of the systems. The significant benefits of $PI^{\lambda}D^{\mu}$ are that it provides the improved regulator of dynamical structures, that are designated through the measured models of FOPID. Additionally, the statistics of $PI^{\lambda}D^{\mu}$ is less penetrating while at the time of system fluctuates. Fig. 3 illustrates the flow diagram of the FOPID controller.

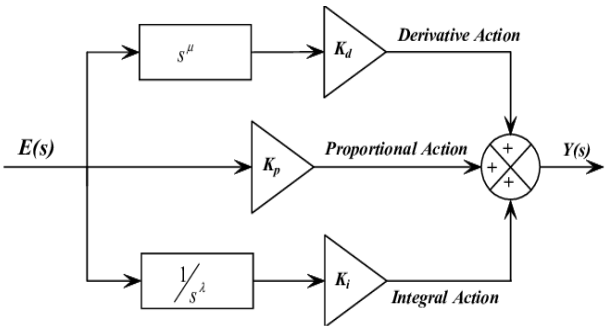

Figure. 3 Flow diagram of FOPID controller

The $PI^{\lambda}D^{\mu}$ with its transfer function is specified through the following Eq. (16) and (17).

$$C(S) = \frac{U(S)}{E(S)} = K_p + Ki\, S^{-\lambda} + K_d\, S^{\mu} \tag{16}$$

$$G_c(s) = \frac{U(s)}{E(s)} = K_p + K_i \frac{1}{S} + K_d S^{\mu}, (\lambda, \mu > 0) \tag{17}$$

Finally, the control signal $U(t)$ is designated by the following Eq. (18),

$$U(t) = K_p e(t) + K_i D^{-\lambda} e(t) + K_d D^{\mu} e(t) \tag{18}$$

Where positive real numbers are stated as $\lambda\, and\, \mu$, proportional, integral and derivative gain constants are described as K_p , K_i and K_d correspondingly. Even by selecting λ = 1 and μ = 1, a conventional PID controller is achieved. Even though, by relating μ = 0, λ = 1, and μ = 1, λ = 0 both the traditional PI and PD controllers are achieved better results. But the FOA-FOPID provides the improvement in all the performance parameters over a standard PID controller. The proposed FOA-FOPID controller is highly suitable for application in all types of hybrid vehicles.

4. Results and discussion

In this research, the effectiveness of the FOA-FOPID technique with a bidirectional DC-DC converter is shown through MATLAB/Simulink simulation. The results have shown that the proposed method gives a better voltage response and the system performance is improved. The innovation of this BDDCDC circuit concept deceits in the scheme of proposed FOA-FOPID is to monitor the samples values with and without including load in calculation to minimalizing the preliminary overshoot.

4.1 Open-loop BDDCDC with C-filter

Here, the physical model is obtained for the designed DC-DC converter circuit. The ideal model

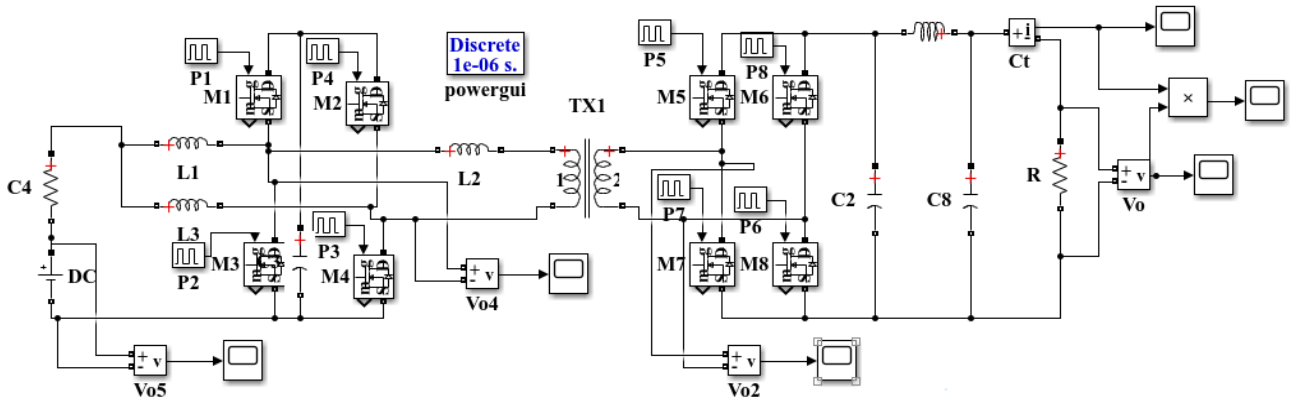

Figure. 4 Simulink model of BDDCDC by C-filter

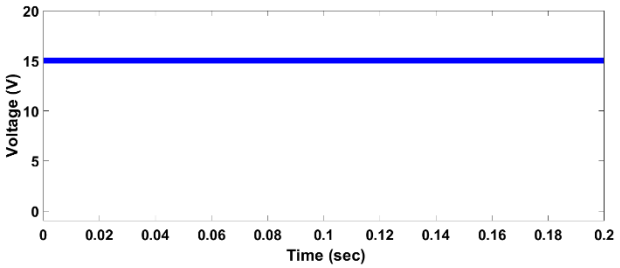

Figure. 5 Input voltage

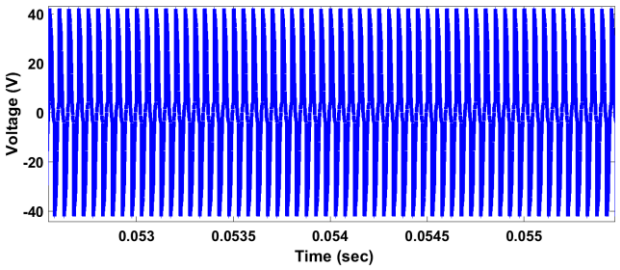

(a)

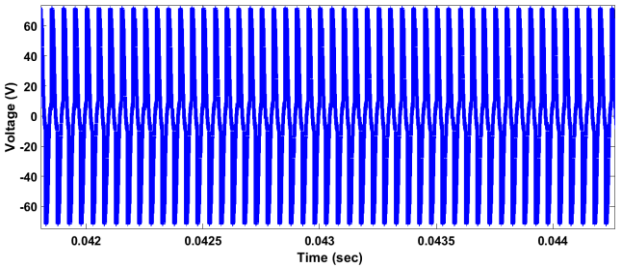

(b)

Figure. 6 (a) Primary voltage of transformer and (b) Secondary voltage of transformer

of bidirectional DC-DC converter is considered for simplifying the complexity of modelling. The Circuit diagram of BDDCDC through C-filter is outlined in Fig. 4. The converter is made with few energy storage elements such as 8 n-channel MOSFETs and 8 diodes, capacitors, inductors and resistances. During switching process MOSFET and diode work compliment to one another i.e. When MOSFET is ON

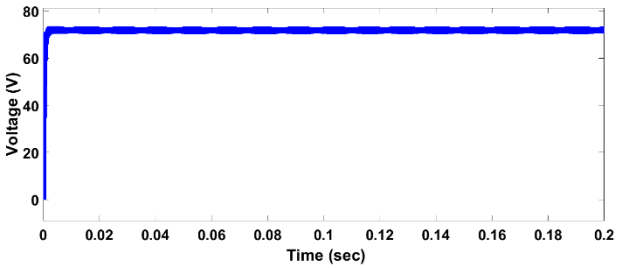

(a)

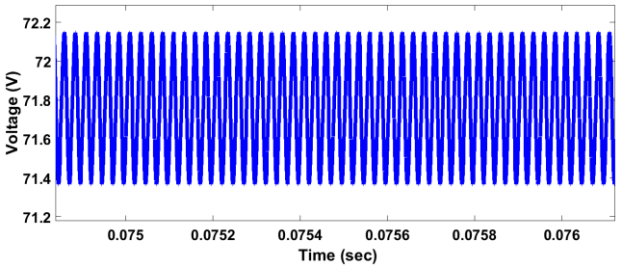

(b)

Figure. 7 (a) R-load voltage and (b) Ripple voltage at R-load

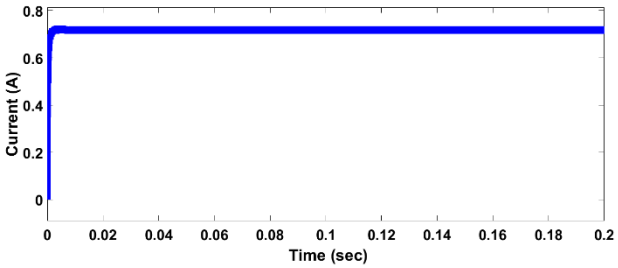

Figure. 8 Current over R-load

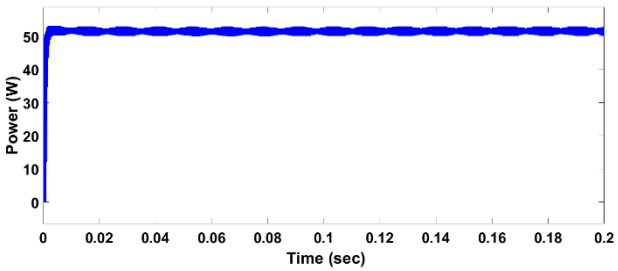

Figure. 9 Output power

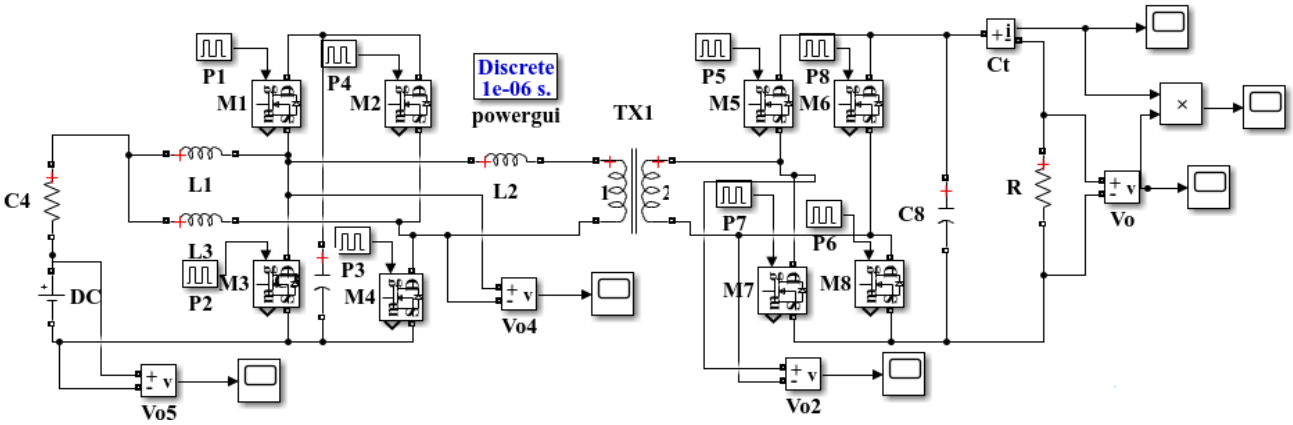

Figure. 10 Simulink model of bi-directional dc-dc converter with C-filter

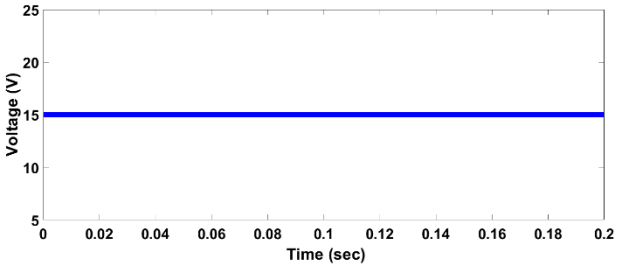

Figure. 11 Input voltage

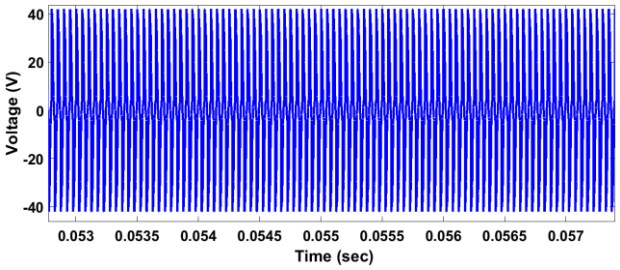

(a)

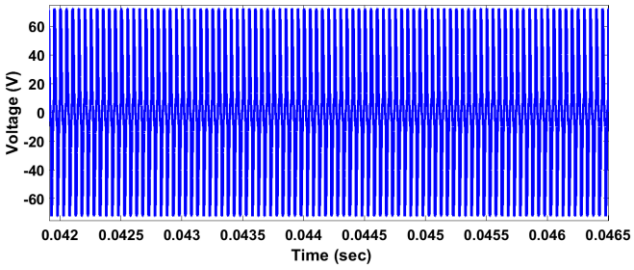

(b)

Figure. 12 (a) Primary voltage of transformer and (b) Secondary voltage of transformer

diode is OFF and when diode is ON, MOSFET is OFF at a given interval of time. The Input Voltage is delineated in Fig. 5 and its range is 15V. The transformer primary voltage is obtained as 40V and transformer secondary voltage is obtained as 71V which is illustrated in Fig. 6. Voltage value across R-load is attained as 70V and Ripple Voltage across R load is attained as 72.1V which is displayed in Fig. 7. Current through R-load is outlined in Fig 8 with 0.75A value. Fig. 9 displays the output resultant power with a range of 50W.

4.2 Open-loop BDDCDC with π-filter

The Circuit diagram of BDDCDC with π-filter is delineated in Fig. 10. Fig. 11 illustrates the input Voltage with a range of 15V. The transformer primary Voltage is attained as 40V and transformer secondary voltage is attained as 71V which is displayed in Fig. 12. The voltage across R-load is determined as 71V, Fig. 13 illustrates the ripple voltage of R-load with a range of 72.1V. Fig. 14 represents the current present at R-load with a range of 0.75A. Fig. 15 illustrates the resultant output power of 50W.

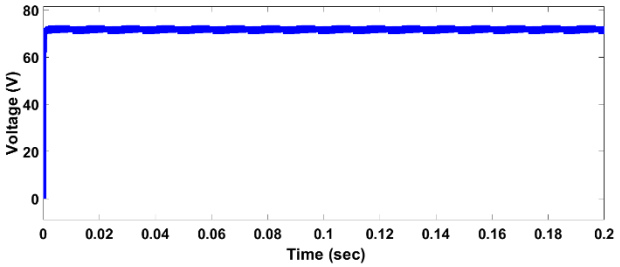

(a)

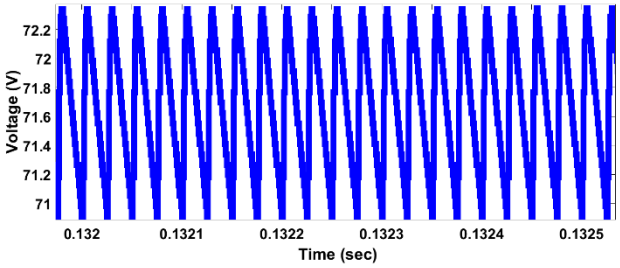

(b)

Figure. 13 (a) R-load voltage and (b) Ripple voltage at R-load

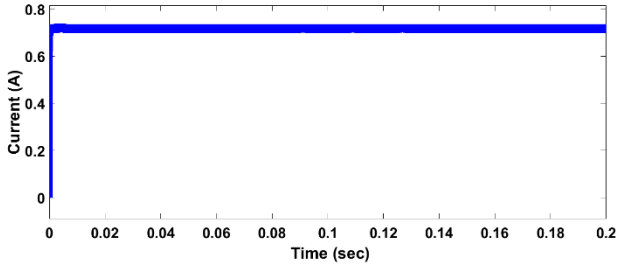

Figure. 14 Current at R-load

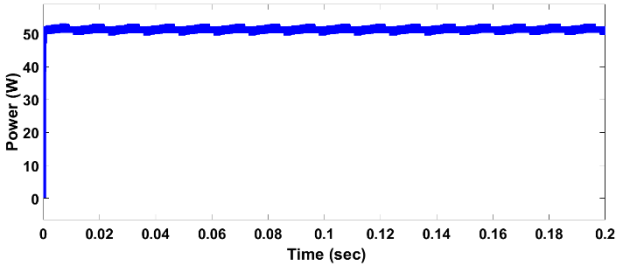

Figure. 15 Output power

Table 2. Assessment of output voltage-ripple

Design of converter	Ripple Voltage
C-Filter	1.2V
Π-Filter	0.7V

Table 2 displays the assessment of output voltage ripple by using the C-filter and π-filter of a bidirectional DC-DC converter. By using π Filter, voltage ripple is condensed from 1.2V to 0.7V. Therefore, the result signifies that the bidirectional DC-DC with Π-Filter is much better than the C-filter design.

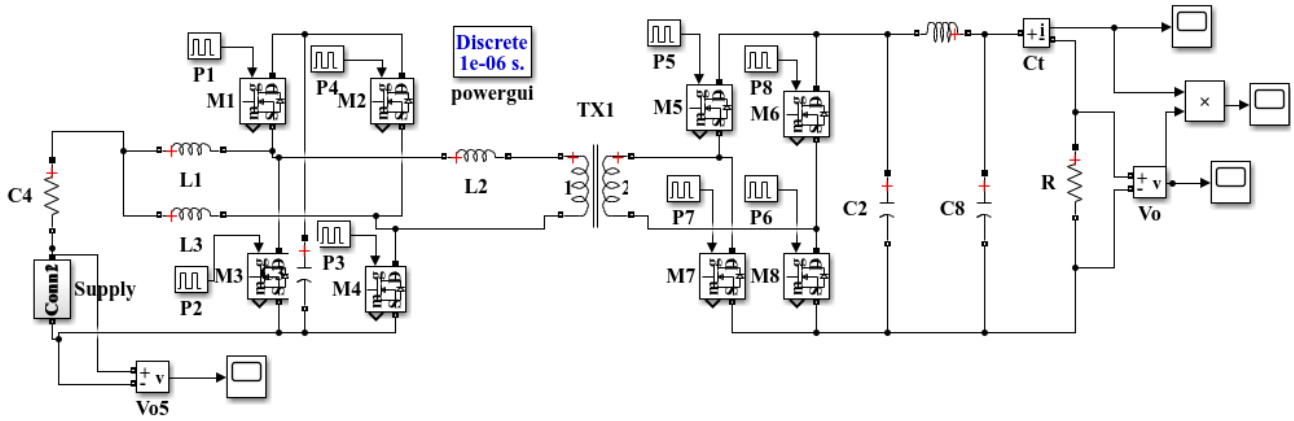

Figure. 16 Circuit diagram of BDCDCDC with source disturbance

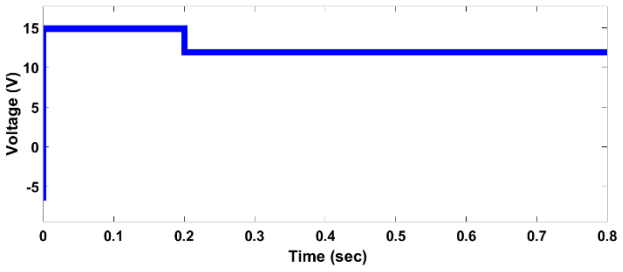

Figure. 17 Input voltage

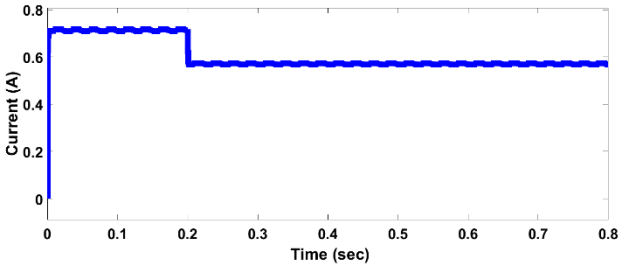

(b)

Figure. 18 (a) Voltage at R-load and (b) Current at R-load

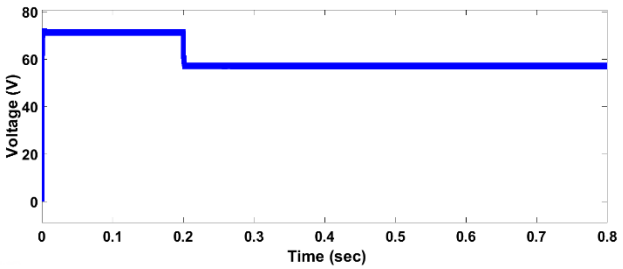

(a)

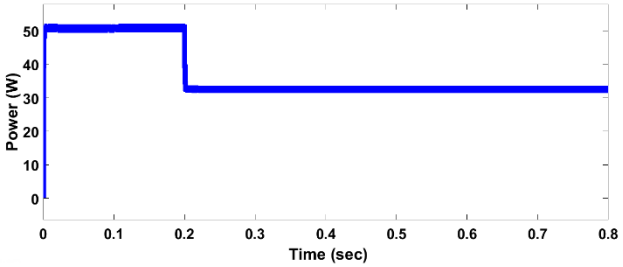

Figure. 19 Output power

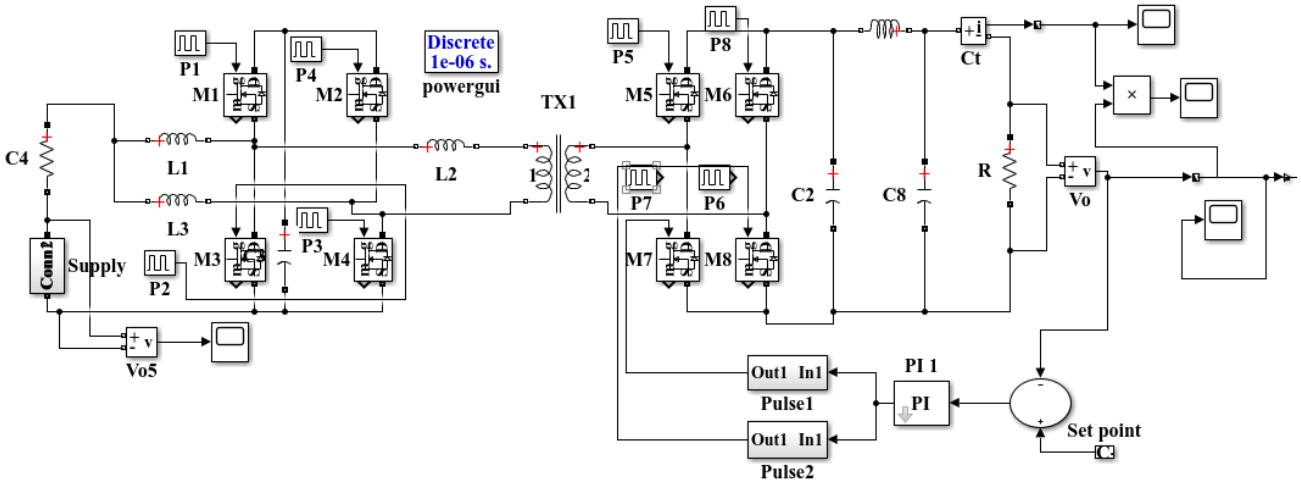

Figure. 20 Simulink model of PI controller with closed loop DC-DC converter

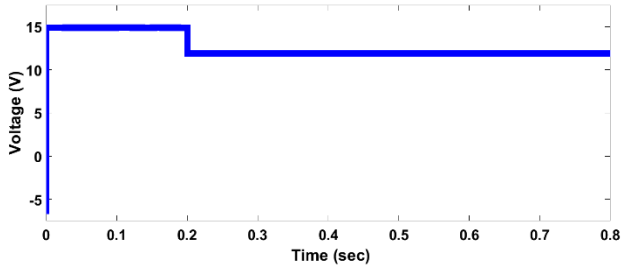

Figure. 21 Input voltage

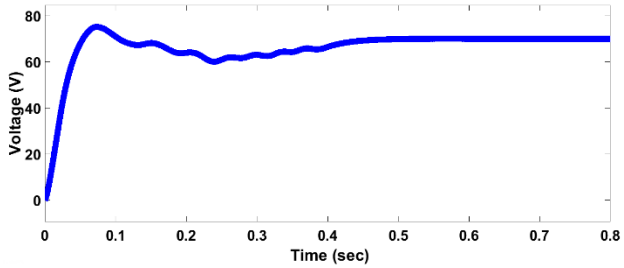

(a)

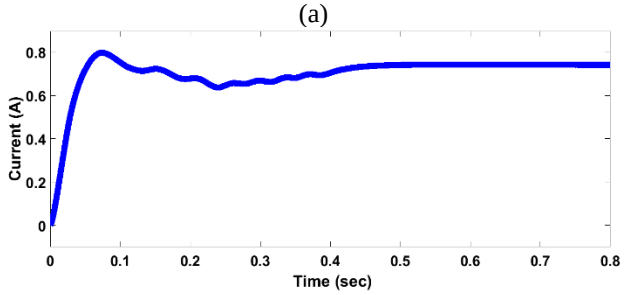

(b)

Figure. 22 (a) Voltage and (b) Current

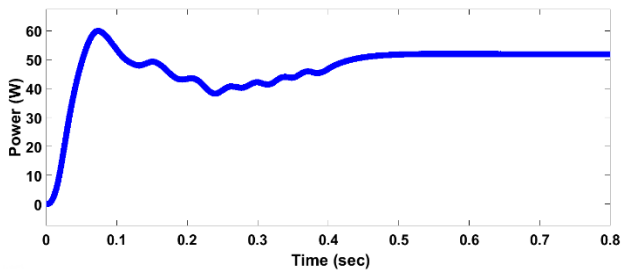

Figure. 23 Output power

4.3 Open-loop BDDCDCD with source disturbance

Fig. 16 illustrates the Circuit diagram of BDDCDC with source disturbance.

Fig. 17 represents the voltage at input side with a range of 12V. Voltage value across R-load is calculated as 60V and Fig. 18 illustrates that current across R-load with 0.6A value. Fig. 19 demarcated the resultant output power of 35W.

4.4 Closed loop BDDCDC with PI

Fig. 20 illustrates the Simulink model of closed loop BDDCDC through PI controller.

Fig. 21 illustrates the 12V voltage at input side. The voltage across R-load is obtained & its value is 67V whereas the current occurs at R-load is determined with 0.78A which is illustrated in Fig. 22. Fig. 23 demarcates the resultant output power of 56W.

4.5 Closed loop BDDCDC with FOPID

The proposed research suggests a policy of the FOA-FOPID controller for designed bidirectional converter. The major aim of this research contains mostly in the scheme of FOA-FOPID response to achieve optimal time domain stipulations in which errors has been minimalized. In addition, the controller constraints of PID are acknowledged. It can be accomplished over and done with fractional order procedure. The Simulink model of bi-directional DC-DC converter along with the fractional order to assess the objective function which outcomes through robust FOA-FOPID transient response. Fig. 24 shows the Simulink model of closed loop BDDCDC by FOA-FOPID controller.

Fig. 25 illustrates the 12V voltage at input side. Voltage across R-load is attained as 67V and the

current through-R-load is attained & its value is 0.78A which is illustrated in Fig. 26. Fig. 27 demarcates the resultant output power of 56W.

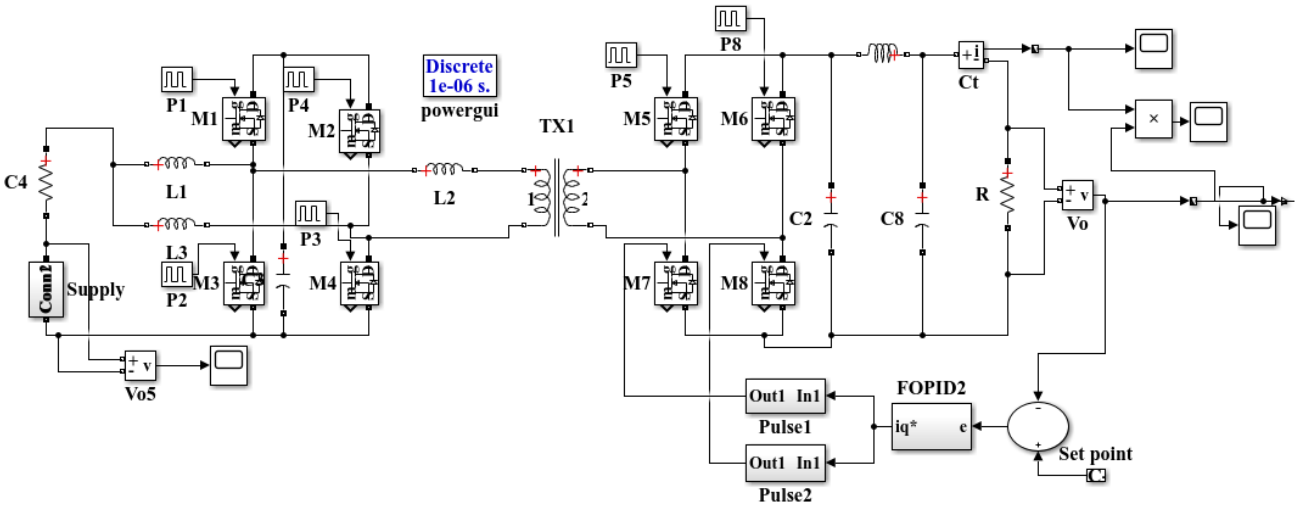

Figure. 24 Simulink model of proposed FOPID under closed-loop BDDCDC

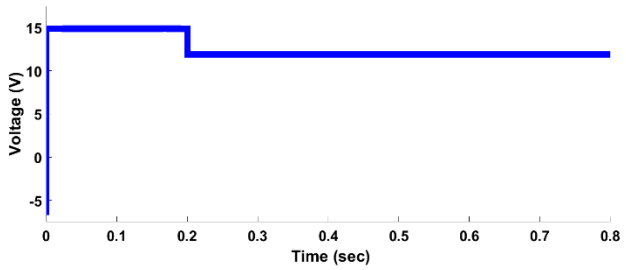

Figure. 25 Input voltage

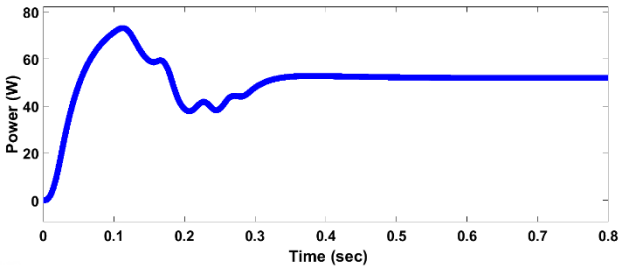

Figure. 27 Output power

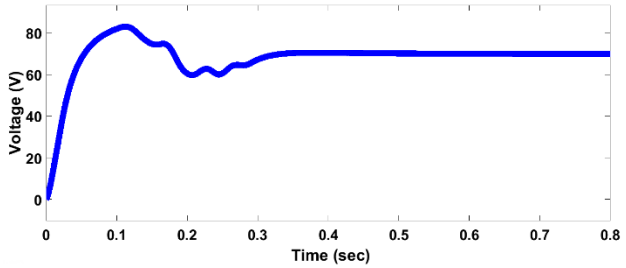

(a)

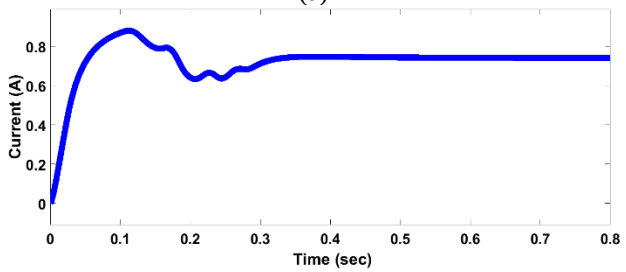

(b)

Figure. 26: (a) Voltage across R-load (b) Current across R-load

Table 3. Assessment of proposed FOA-FOPID with existing PI controller

Controller	T_r	T_p	T_s	E_{ss}
PI	0.22	0.27	0.45	1.6
FOA-FOPID	0.21	0.24	0.33	1.1

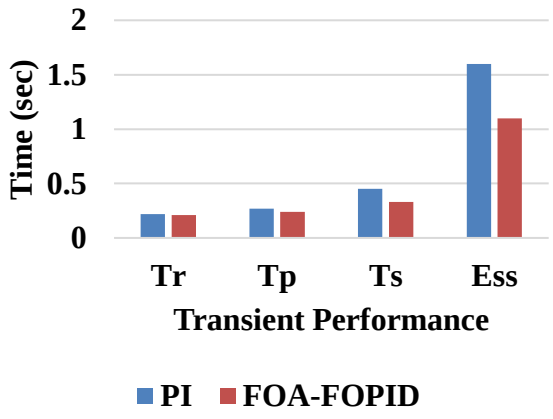

Figure. 28 Graphical view of time domain factors using PI & FOA-FOPID

Table 4. Comparison for steady state error

Loading Conditions	Parameters	ANFIS Controller [17]	GWO Controller [20]	Proposed FOA-FOPID
Full Load (100 %)	Steady State Error (%)	0.16	-	0.12
	Rise time (s)	0.27	-	0.22
	RMSE	-	1.0683	0.9727

Table 5. Transient response of settling time and rise time

Loading Condition	Parameters	MGA-FOPID [18]	PID Controller [15]	Proposed FOA-FOPID Controller
Full Load (100 %)	Settling Time (s)	0.80	0.45	0.33
	Rise time (s)	0.63	0.22	0.21

Table 6. Transient analysis

Constraints	DPCT method [16]	Proposed FOA-FOPID
Peak time (s)	0.312	0.289
Settling Time (s)	0.431	0.311
Peak Overshoot (%)	0.013	0.008

4.6 Comparative analysis

In [17], BLDC drives are controlled with Adaptive Neuro Fuzzy Inference Control (ANFIS). From the outcomes, under variable load condition, ANIFS achieved the steady state error of 0.16 % and it takes 0.27 sec rise time for 3000 speed reference. But, proposed FOA-FOPID provides steady state error of 0.12 % which is better when contrasted with ANFIS. Furthermore, it can quickly make the framework stable with rise time of 0.21 sec.

To assess the presence of the BLDC engine, various estimations are taken. The transient presentation results for the Conventional PID, ANFIS and GWO regulator of BLDC Motor are displayed in Table 3. From the Table 4, Root Mean Square Error (RMSE) values are obtained from the simulation model. The proposed FOA-FOPID controller produces less RMSE of 0,9727 when compared with existing GWO method [20]. Accompanying qualities such as rise time, overshoot, steady-state error, settling time, and stability are considered. From the Simulation, BLDC motor speed control of FOA-FOPID controller had better performance than MGA-FOPID [18] which is tabulated in Table 5.

From Table 5, it is clear that overshoot time in PID controller is high when compared with that of MGA-FOPID [18] and PID [15]. The existing MGA-FOPID has the settling time (0.80) and rise time (0.63), where PID has 0.45 sec & 0.22 sec which are more when compared with proposed FOA-FOPID controller transient performance.

Table 6 shows the transient analysis of existing methods. Table 6 clearly shows that the proposed FOA-FOPID delivered a better response when compared with Dynamic Power Containment Technology (DPCT) [25]. The existing DPCT achieves the peak time (0.312), peak overshoot (0.013), settling time (0.431) which is less when compared with proposed FOA-FOPID controller which attained the results in a quicker period. Simulation results showing that proposed FOA-FOPID provides lesser overshoot (0.008%), quicker settling time (0.311s) and peak time (0.289s).

The existing controller achieves the transient stability which is less when compared with proposed FOA-FOPID controller which attained the results in a quicker period. Simulation results showing that FOA-FOPID provides quicker settling time (0.33s) and rise time (0.21s). The performance of the two controllers is compared based on various control system parameters such as steady-state error, rise time, peak overshoot and settling time. It is found that the control concept with the proposed FOA-FOPID controller outperforms the classical controller in most of aspects.

5. Conclusion

In this research study, BDDCDC with C-filter and Π-Filter are simulated. The outcome proves that the BDDCDC with π -Filter is superior to BDDCDC with C-filter. The open-loop and closed-loop BDDCDC with FOA-FOPID are demonstrated, analysed, and simulated. By using FOA-FOPID, the rise time of FOPID is condensed from 0.22Sec to 0.21Sec, Steady-state error is reduced from 1.6V to 1.1V, where the settling time is condensed from 0.45Sec to 0.33Sec, also the peak time is condensed from 0.27 Sec to 0.24 Sec. Henceforth the result signifies that the CLBDDCDC with FOA-FOPID controller is much better than CLBDDCDC with PI controller. This research can be extended by modifying the topology of the CLBDDCDC with recent optimization techniques.

Conflicts of Interest

The authors declare no conflict of interest.

Author Contributions

The paper background work, conceptualization, methodology, dataset collection, implementation, result analysis and comparison, preparing and editing draft, visualization have been done by 2nd, 3rd and 4th author. The supervision, review of work and project administration, have been done by 1st author.

References

[1] L. S. Yang and T. J. Liang, "Analysis and implementation of a novel bidirectional DC–DC converter", *IEEE Transactions on Industrial Electronics*, Vol. 59, No. 1, pp. 422-434, 2011.

[2] C. C. Lin, L. S. Yang, and G. W. Wu, "Study of a non-isolated", *IET Power Electronics*, Vol. 6, No. 1, pp. 30-37, 2013.

[3] R. T. Naayagi, A. J. Forsyth, and R. Shuttleworth, "High-power bidirectional DC–DC converter for aerospace applications", *IEEE Transactions on Power Electronics*, Vol. 27, No. 11, pp. 4366-4379, 2012.

[4] H. Ardi, A. Ajami, F. Kardan, and S. N. Avilagh, "Analysis and implementation of a nonisolated bidirectional DC–DC converter with high voltage gain", *IEEE Transactions on Industrial Electronics*, Vol. 63, No. 8, pp. 4878-4888, 2016.

[5] H. Ardi, R. R. Ahrabi, and S. N. Ravadanegh, "Non-isolated bidirectional DC–DC converter analysis and implementation", *IET Power Electronics*, Vol. 7, No. 12, pp. 3033-3044, 2014.

[6] Y. P. Hsieh, J. F. Chen, L. S. Yang, C. Y. Wu, and W. S. Liu, "High-conversion-ratio bidirectional dc–dc converter with coupled inductor", *IEEE Transactions on Industrial Electronics*, Vol. 61, No. 1, pp. 210-222, 2013.

[7] B. Zhao, Q. Song, W. Liu, and Y. Sun, "Overview of dual-active-bridge isolated bidirectional DC–DC converter for high-frequency-link power-conversion system", *IEEE Transactions on Power Electronics*, Vol. 29, No. 8, pp. 4091-4106, 2013.

[8] J. B. Baek, W. I. Choi, and B. H. Cho, "Digital adaptive frequency modulation for bidirectional DC–DC converter", *IEEE Transactions on Industrial Electronics*, Vol. 60, No. 11, pp. 5167-5176, 2012.

[9] R. J. Wai, R. Y. Duan, and K. H. Jheng, "High-efficiency bidirectional dc–dc converter with high-voltage gain", *IET Power Electronics*, Vol. 5, No. 2, pp. 173-184, 2012.

[10] R. P. Twiname, D. J. Thrimawithana, U. K. Madawala, and C. A. Baguley, "A new resonant bidirectional DC–DC converter topology", *IEEE Transactions on Power Electronics*, Vol. 29, No. 9, pp. 4733-4740, 2013.

[11] T. J. Liang and J. H. Lee, "Novel high-conversion-ratio high-efficiency isolated bidirectional DC–DC converter", *IEEE Transactions on Industrial Electronics*, Vol. 62, No. 7, pp. 4492-4503, 2014.

[12] K. B. Liu, C. Y. Liu, Y. H. Liu, Y. C. Chien, B. S. Wang, and Y. S. Wong, "Analysis and controller design of a universal bidirectional DC-DC converter", *Energies*, Vol. 9, No. 7, p. 501, 2016.

[13] A. Tong, L. Hang, G. Li, X. Jiang, and S. Gao, "Modeling and analysis of a dual-active-bridge-isolated bidirectional DC/DC converter to minimize RMS current with whole operating range", *IEEE Transactions on Power Electronics*, Vol. 3, No. 6, pp. 5302-5316, 2017.

[14] A. Chub, D. Vinnikov, R. Kosenko, E. Liivik, and I. Galkin, "Bidirectional DC–DC converter for modular residential battery energy storage systems", *IEEE Transactions on Industrial Electronics*, Vol. 67, No. 3, pp. 1944-1955, 2019.

[15] Kumar, Brajesh, S. K. Swain, and N. Neogi, "Controller design for closed loop speed control of BLDC motor", *International Journal on Electrical Engineering and Informatics* 9, No. 1, 2017.

[16] S. Subramanian, R. Mohan, S. K. Shanmugam, N. Bacanin, M. Zivkovic, and I. Strumberger, "Speed control and quantum vibration reduction of Brushless DC Motor using FPGA based Dynamic Power Containment Technique", *Journal of Ambient Intelligence and Humanized Computing*, pp. 1-15, 2021.

[17] H. Suryoatmojo, D. R. Pratomo, M. R. Soedibyo, D. C. Riawan, E. Setijadi, and R. Mardiyanto, "Robust Speed Control of Brushless Dc Motor Based on Adaptive Neuro Fuzzy Inference System for Electric Motorcycle Application", *International Journal of Innovative Computing Information and Control*, Vol. 16, No. 2, pp. 415-428, 2020.

[18] K. Vanchinathan, K. R. Valluvan, C. Gnanavel, and C. Gokul, "Design methodology and experimental verification of intelligent speed controllers for sensor less permanent magnet Brushless DC motor: Intelligent speed controllers for electric motor", *International Transactions on Electrical Energy Systems*, Vol. 31, No. 9 p. e12991, 2021.

[19] M. D. A. Mawlawe, M. A. Ahmed, and M. K. Husein, "Transcribing the Fuzzy Logic Technique for Buck-Boost Dc-Dc Converter",

Journal of Engineering Science and Technology, pp. 1-9, 2021.

[20] J. A. Leon, C. C. Palacios, V. S. Carlos, E. H. Perez, and E. X. Garcia, "Particle Swarm Optimization, Genetic Algorithm and Grey Wolf Optimizer Algorithms Performance Comparative for a DC-DC Boost Converter PID Controller", *Advances in Science, Technology and Engineering Systems Journal*, Vol. 6, No. 1, pp. 619-625, 2021.